Industrial Engineering Journal
ISSN: 0970-2555
Volume : 52, Issue 2, No. 1, February : 2023

AN OPTIMIZED DEEP LEARNING ALGORITHM FOR SPLICING DETECTION AND LOCALIZATION IN DIGITAL IMAGES

Thote NansiNeitngale PG scholar,
pakki Sridevi, Allu Venkateswara Rao, Associate professor,
Department of ECE, MIRACLE educational society group of institutions, Bhogapuram, Vizianagaram.India : nansi1201@gmail.com

ABSTRACT

Digital images are very necessary for various fields because of the availability of software and applications, which can create the images as looking reality. In the digital world, image modification is very easy because of the availability of several software applications. These are helped to manipulate the original image. Manipulated image very close to the natural image. Image splicing detection techniques have been developed to ensure whether the image content is modified after it was acquired. Image splicing detection would have huge impact in various application domains such as, crime investigation and detection, fashion industry, scientific journals, insurance claim processing, law enforcement, medical imaging, surveillance system and many others. Hence, a new optimized algorithm Generalized Approximate Reasoning based Intelligence Control (GARIC) with regression rules for feature extraction, feature matching and post processing. Ithas been implemented with reduced multi-dimensional scaling features to discover the spliced image regions which are blurred, brightness altered and color reduced with different levels. So that we have developed an optimized deep learning algorithm to detect spliced region effectively. Here, the Action selection network (ASN) is a 5-layer network used to distinguishes the spliced image tampering. This method is simulated using Python and the results prove the performance of an innovative method. Moreover, the obtained results are compared with recent existing approaches.

Keywords:*spliced images, Natural images, Neural networks, GARIC architecture.*

I. INTRODUCTION

Image forgery is a sensitive issue and we have to take utmost care. With the swift reclamation of digital image processing scheme and the emerging growth of digital camera,software and forgery tools, tampering an image becomes much easier and increasesgradually. Resampling, splicing, object removal and copy-move forgery are the main methods to cause manipulations in images. Hence, we need an efficient, accurate and robust tampering detection methods to detect digital images. Human visual system perceives the pictorial information faster than any other kind of information. According to biologists, 75% of information perceived by the human brain is by visual activity. Images are generally used as major source of information for effective communication. An extended application based on the images includes security and authentication. However, the reliability of image is questionable due to the powerful and low-cost image editing technologies which facilitate to acquire and manipulate digital images [1]. These technological advancements laid a path to the researchers for analyzing splices of images in image centric applications. Two primary questions need to be addressed by these researchers:

(1) Whether the images are original or manipulated

(2) Whether images captured using acquisition devices or fabricated images

To answer these questions image source identification and digital image splicing detection techniques got important in digital image world. Image source identification is interesting research even for identifying devices which is used to capture the image in order to discriminate the image is acquired using a

digital device or it is a computer-generated image [2]. Forensics analysis of digital image contents is a new field of research which facilitates to ensure the authenticity of digital images

An overview of different types of image manipulations is presented at first, followed by techniques in image forgery detection. One important type of image forgery is copy-move forgery. Because of its popularity and opportunities to find research objectives in the detection of copy-move forgery, many techniques have been developed in this area. This thesis concentrates in developing methods for detection of copy-move type image forgery.

Images can be manipulated in many ways and Kakar [2012] has classified these image manipulations into four; namely, copy-move, splicing, application of image processing operations, false captioning etc. Image manipulations are termed in this thesis as image splicing Ing or image forgery. Image splicing [13] is the most commonly performed type of image forgery. In this type of forgery, a region in an image is hidden by pasting another region, copied from some other location of the same image, over it. This type of forgery is done intentionally to hide the presence of some object or a person or to duplicate something in an image. Copy-move forgeries [3] are also referred to as copy paste forgery. Splicing or photomontage is created by combining two or more images to convey false information. Many examples of this type of photo forgery can be seen in history and nowadays in social media. Photos can also be manipulated using some image processing operations like changing the hue, colour, skin tone etc. These types of manipulations do not hide or add any information, but it betrays the observer at a psychological level. These types of manipulations are seen in the media and movie industry. Reality can be distorted even without touching the photo. This type of forgery comes under false captioning, where the caption of the image is provided in a way that misleads the observer. Sometimes the metadata associated with the image is also altered. 16 AI based techniques are usually employed in detecting these types of forgeries. The different types of image forgery [4] and the mechanism to handle each of them are well stated in a study by Devi Mahalakshmi et al. [2012].

Images are processed by spatial and frequency domain methods. Spatial domain methods operate directly on the image pixels and incurred more computation which makes the image processing task a complex one. Frequency domain methods transform the image in to frequency domain and perform operations on transformed image. After processing, the image is transformed back to original image by means of inverse transform. Transformation function provides some additional or hidden information and it is easyto solve than the original function.Image transformationfunctions are extensively applied in pre-processing, image compression or data reduction and feature extraction.

II. EXISTING METHODS

Inthissection,wediscuss various image transformation techniques, their applications and limitations. A new block-based approach has been introduced. The proposed method overcome the pitfalls in Exhaustive search and Autocorrelation methods which compares every image segment with all other image segment to identify similar region in an image. This approach makes use of Discrete Cosine Transform (DCT) co-efficient to detect most familiar and decisive type of splicing called copy-move. Primary objective of this method is to exactly detect and locate very small and multiple spliced regions even the spliced regions are flipped, enhanced or retouched.

❖ Role of Transformation in splicing Detection

Various transformation methods have already in use. Few important transformation techniques have been discussed as follows,

1. Fourier Transform

Fourier transform expresses non-periodic, even functions with finite durations as an integral of sines / cosines multiplied by a weighting function. Fourier transformation

Industrial Engineering Journal
ISSN: 0970-2555
Volume : 52, Issue 2, No. 1, February : 2023

function is completely recovered back to the spatial domain through inverse process without loss of any information.

(a) The One-Dimensional Fourier Transform

If f(x) is a continuous function of real variable *x*, The Fourier transform of *f(x)* is computed with the formula,

$$F[f(x)] = F(u) = \int_{-\infty}^{\infty} f(x).e^{-j2\pi ux}\, dx$$

Where $j = \sqrt{-1}$, $e^{-j2\pi ux} = cos\ 2\pi ux - jsin2\pi ux$ is Euler's formula and *u* is a frequency variable.

Inverse Fourier transformation is obtained using the formula,

$$F^{-1}[F(u)] = f(x) = \int_{-\infty}^{\infty} F(u).e^{-j2\pi ux}\, du$$

The above two equation exist only if *f(x)* is continuous

(b) The Two-Dimensional Fourier Transform

If the one dimensional Fourier Transform is extended to two variable function *f(x, y)* than, the two dimensional forward Fourier transform of *f(x, y)* is computer as,

$$F[f(x,y)] = F(u,v) = \int_{-\infty}^{\infty}\int_{-\infty}^{\infty} f(x,y).e^{-j2\pi(ux+vy)}\, dxdy$$

Where, *u* and *v* are frequency variables

Two-dimensional inverse Fourier transform is obtained using the formula,

$$F^{-1}[F(u,v)] = f(x,y) = \int_{-\infty}^{\infty}\int_{-\infty}^{\infty} F(u,v).e^{-j2\pi(ux+vy)}\, dudv$$

1.1 Discrete Fourier Transform (DFT)

Discrete Fourier Transforms (DFT) exposes periodicities and strength of periodic components in the input signals. In DFT independent variables are discrete and always there exist an inverse for forward DFT [6].

(a) The One-Dimensional DFT

The Fourier transform of discrete function *f(x)* with single variable is calculated with the formula,

$$F(u) = \frac{1}{N}\sum_{x=0}^{N-1} f(x).e^{-\frac{j2\pi ux}{N}}$$

Where *u*=0,1,2……*N-1*

The inverse transformation is obtained using the formula,

$$f(x) = \sum_{u=0}^{N-1} F(u).e^{\frac{j2\pi ux}{N}}$$

Where, x=0, 1, 2……N-1

(b) The Two-Dimensional DFT

Discrete Fourier Transformation of a function (image) *f(x, y)* of size *MN* is specified by the equation,

$$F(u,v) = \frac{1}{M.N}\sum_{x=0}^{M-1}\sum_{y=0}^{N-1} f(x,y).e^{-j2\pi\left(\frac{ux}{M}+\frac{vy}{N}\right)}$$

For u=0, 1, 2 ...M-1 and *v=0, 1, 2……N-1*

The inverse DFT is obtained with the formula

$$f(x,y) = \sum_{u=0}^{M-1}\sum_{v=0}^{N-1} F(u,v).e^{-j2\pi\left(\frac{ux}{M}+\frac{vy}{N}\right)}$$

Where *x=0, 1, 2…..M-1* and *y=0, 1, 2……N-1*

2. Walsh Transform

It is a real transform consist series expansion for basic functions whose values are +1 or - 1 hence, it requires less computer memory than Fourier transform. Walsh transformation is mainly used in multiplexing, in which several data is simultaneously transmitted without the need of high energy packing capability [8].

(a) One-dimensional Walsh Transform

The one-dimensional Walsh transformation of a function f(x) is denoted by *WT (u)* and it is calculated using the formula,

$$WT(u) = \frac{1}{N}\sum_{x=0}^{N-1} f(x)\prod_{i=0}^{n-1}(-1)^{[b_i(x)b_{n-1-i}(u)}$$

Where, *g(x, u)* is the 1-D forward Walsh kernel and it is given by,

$$g(x,u) = \frac{1}{N}\prod_{i=0}^{n-1}(-1)^{[b_i(x)b_{n-1-i}(u)}$$

where, $N = 2^n$ and $b_x(z) - x^{th}$

Inverse 1D Walsh Transform is expressed as,

$$f(x) = \sum_{u=0}^{N-1} WT(u)\prod_{i=0}^{n-1}(-1)^{[b_i(x)b_{n-1-i}(u)}$$

The 1-D Inverse Walsh kernel is given by,

$$h(x,u) = \prod_{i=0}^{n-1}(-1)^{[b_i(x)b_{n-1-i}(u)}$$

Industrial Engineering Journal
ISSN: 0970-2555
Volume : 52, Issue 2, No. 1, February : 2023

(b) Two-Dimensional Walsh transform

The 2-D Walsh transform is separable and symmetric. Hence, it is obtained by sequence of two one dimensional Walsh transforms. It is in the form of square waves and implemented more efficiently in a digital environment than the exponential basis functions of Fourier transform. Forward Walsh Transform is obtained by straight modification of FFT which uses successive doubling method.

$$WT(u,v)=\frac{1}{N}\sum_{x=0}^{N-1}\sum_{y=0}^{N-1}f(x,y)\prod_{i=0}^{n-1}(-1)^{[b_i(x)b_{n-1-i}(u)+b_i(y)b_{n-1-i}(v)]}$$

Where, 2-D forward Walsh kernel g x, y, u, v is given by,

$$f(x,y)=\frac{1}{N}\sum_{u=0}^{N-1}\sum_{v=0}^{N-1}WT(u,v)\prod_{i=0}^{n-1}(-1)^{[b_i(x)b_{n-1-i}(u)+b_i(y)b_{n-1-i}(v)]}$$

Where, 2-D inverse Walsh kernel h x, y, u, v is given by,

$$h(x,y,u,v)=\frac{1}{N}\prod_{i=0}^{n-1}(-1)^{[b_i(x)b_{n-1-i}(u)+b_i(y)b_{n-1-i}(v)]}$$

3. The HADAMARD Transform

HADAMARD transform is well suited for digital signal processing because the basic vectors of this transform take only the values +1 and -1. Therefore, no multiplications are required in the transform calculation. It is real, symmetric and orthogonal transform which reduce number of additions and subtractions from N2 to Nlog2N. Recursive relation is an important property in which HADAMARD matrix of any size is computed from the small initial HADAMARD matrix. This transform is widely applied in the areas such as image compression, filtering and design.

(a) The one-dimensional HADAMARD Transform

The 1-D forward HADAMARD transform is calculated using the formula,

$$HT(u)=\frac{1}{N}\sum_{x=0}^{N-1}f(x)(-1)^{\sum_{i=0}^{n-1}b_i(x)b_i(u)}$$

For *u=0….N-1* and

$$g(x,u)=\frac{1}{N}(-1)^{\sum_{i=0}^{n-1}b_i(x)b_i(u)}$$

is the 1-D forward HADAMARD Kernel, *N=2n* ,

$b_x(z)$ – x^{th}bit in the binary representation of z

The inverse HADAMARD transform is obtained by the formula,

$$f(x)=\sum_{u=0}^{N-1}HT(u).(-1)^{\sum_{i=0}^{n-1}b_i(x)b_i(u)}$$

Where *x=0, 1…N-1* and *h (x, u)* = $(-1)^{\sum_{i=0}^{n-1}b_i(x)b_i(u)}$ is 1-D inverse HADAMARD kernel.

(b) The two-dimensional HADAMARD Transform

2-D HADAMARD transform is calculated using the formula,

$$HT(u,v)=\frac{1}{N}\sum_{x=0}^{N-1}\sum_{y=0}^{N-1}f(x,y)\,(-1)^{\sum_{i=0}^{n-1}b_i(x)b_i(u)+b_i(y)b_i(v)}$$

Where,

$$g(x,y,u,v)=\frac{1}{N}(-1)^{\sum_{i=0}^{n-1}b_i(x)b_i(u)+b_i(y)b_i(v)}$$

$$f(x,y)=\frac{1}{N}\sum_{u=0}^{N-1}\sum_{v=0}^{N-1}HT(u,v)\,(-1)^{\sum_{i=0}^{n-1}b_i(x)b_i(u)+b_i(y)b_i(v)}$$

Where,

$h(x,y,u,v)=\frac{1}{N}(-1)^{\sum_{i=0}^{n-1}b_i(x)b_i(u)+b_i(y)b_i(v)}$ is the 2-D inverse HADAMARD kernel.

4. The HAAR Transform

The HAAR transform is real, orthogonal and fast transform on N X 1 vector. It can be implemented in O (N) operations. The basic vectors of HAAR [9] matrix are sequentially ordered and used for image edge extraction. This transform exhibit poor energy compaction for images therefore it is not much useful in practice.

5. The SLANT Transform

SLANT transform is developed for monochrome or color image coding. Quality of an image coded by SLANT transform is higher than other unitary transform coded images. It is real, orthogonal and fast transforms which can be implemented in O (Nlog2N) operations on an N X 1 vector. Even though it has better energy compaction property than HAAR transform it is not used in practice [6].

Industrial Engineering Journal
ISSN: 0970-2555
Volume : 52, Issue 2, No. 1, February : 2023

6. KARHUNEN LOEVE (KL) or HOTELLING Transform

The KL transform or HOTELLING transform is also known as eigenvector transform or method of principal components or Discrete KL transform. It is based on the statistical properties of vector representation. It is very important tool used to evaluate performance and finding performance bounds in image data.

All transformations discussed in the above section have low energy compaction, de-decorrelation property which leads the possibility for redundant data and bundle of energy is associated with many coefficients [7].

❖ Discrete Cosine Transform (DCT)

DCT is the best suitable method to address various issues discussed in previous section. An interesting contribution in this research work is the design and development of new splicing detection method using DCT. The Discrete Cosine Transform or Cosine transform is a fast transform mainly used in image compression. This mathematical transformation technique used to transform the image from spatial domain to frequency domain and attempt to de-correlate the image data after each transform co-efficient are encoded independently. Since DCT kernels are separable and orthogonal the 2D forward and inverse transform can be computed by successive application of 1D-DCT algorithm.

DCT is directly obtained from FFT algorithm and the *N*x*N* DCT is very close to KL transform of first order stationary Markov sequence of length N.

(a) One-dimensional DCT

The one-dimensional DCT coefficients are calculated with the formula,

$$c(u) = \alpha(u)\sum_{x=0}^{N-1} f(x)\cos\left(\frac{(2x+1)u\pi}{2N}\right)$$

Where *u=0, 1, 2…N-1* and

$$\alpha(u) = \begin{cases} \sqrt{\frac{1}{n}} & \text{for } u = 0 \\ \sqrt{\frac{2}{n}} & \text{for } u = 1,2,\dots,N-1 \end{cases}$$

(b) Two-dimensional DCT

$$c(u,v) = \alpha(u)\alpha(v)\sum_{x=0}^{N-1}\sum_{y=0}^{N-1} f(x,y)\left[\cos\left(\frac{(2x+1)u\pi}{2N}\right)\cos\left(\frac{(2x+1)v\pi}{2N}\right)\right]$$

Where *u=0, 1, 2….N-1* and *v=0, 1, 2…..N-1* and

$$\alpha(u) \text{or } \alpha(v) = \begin{cases} \sqrt{\frac{1}{n}} & for\ \ u\ (\text{or})\ v = 0 \\ \sqrt{\frac{2}{n}} & for\ \ u\ (\text{or})\ v = 1,2,..N-1 \end{cases}$$

❖ Existing Method: DCT Based splicing Detection using sub block approach

Architecture of proposed splicing detection method is shown in figure1.

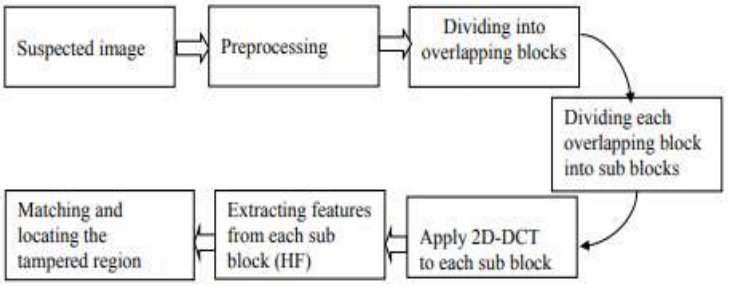

Figure 1: Frame work of proposed splicing detection algorithm

Step 1: Pre-processing: In the first step, the suspected input image I is checked as gray scale or colour image. The colour image is converted in to gray scale using the formula,

I1 = 0.299 R + 0.587 G + 0.114 B

where, R, G, and B are the three colour channels of suspected image.

Step 2: In order to ascertain the spliced region, the pre-processed input image is divided into overlapping blocks of fixed size *b X b*. After series of experiments and comparisons block size is fixed as *8 X 8*. Each overlapping blocks are represented by *OBij*where *i*and *j* indicates starting position of row and column of a particular block. Total number of overlapping blocks should not exceeds *(M-b+1)(N-b+1).*

Industrial Engineering Journal
ISSN: 0970-2555
Volume : 52, Issue 2, No. 1, February : 2023

Where *M, N* denotes the size of the input image and b denotes the block size. This process is illustrated in figure 2.

Step 3: Every overlapping blocks of size *b X b* is further divided into non-overlapping sub blocks of size *NB X NB*.

Step4: Two-Dimensional Discrete Cosine Transformations (2D-DCT) is applied to each non-overlapping sub block to extract the feature vector.

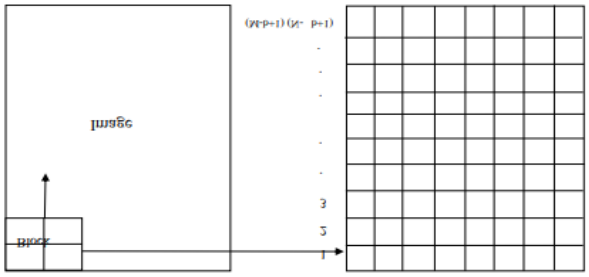

Figure 2: Pixel block scan and matrix representation of proposed algorithm

Step 5: Each sub blocks include both low and high frequency DCT coefficients [9]. The high frequency DCT coefficients from each sub-blocks are extracted and arranged in a two-dimensional matrix (MatHF). Each row of a matrix contains one block coefficients. Lexicographical sorting is applied to the matrix in order to compare the similarity between the blocks. As a result, similar rows are adjacent to each other which help to locate the spliced regions.

Step 6: Every row in a two-dimensional matrix M is compared with all other rows in order to match the similar image blocks. If two rows are similar the algorithm stores the position of identical rows and shift vector (SV) is calculated using the formula,

SV = (SV1, SV2) = (i1 - j1, i2 - j2)

III. ARTIFICIAL NEURALNETWORKS

In the proposed method of Artificial Neural Networks [10], there are two types of classifiers has been performed such as Single Layer Artificial Neural Network Classifier and Optimized Multilayer with Back Propagation Algorithm for detecting the skin MelanocytesBut the Optimized Multilayer with Back Propagation Algorithm is performed better - classification rate of result in Single Layer Artificial Neural Network Classifier.

[1] Reason for selecting Artificial Neural Networks

In our research work, Artificial Neural Network (ANN) is choosing as a classifier for skin Melanocytes Classification because of its architecture. For the mathematical point of view Artificial Neural Network is a dynamic system and also it is able to model as a set of coupled differential equations. The major advantage of using Artificial Neural Network is used such as Neurocomputing, Learning, Adaptability, Robustness, Fault tolerance, Asynchronous. The number of parameters is played a vital part of performance of ANN classifier. These parameters are increasing the percentage rate of accuracy. Basic parameters of ANN classifier are number of Layers involved in the networks, number of neurons performed for each layer, number of iterations, adaptability degree, selecting the non-linearity function, learning algorithm and learning momentum, immunity of noise and so on[8].

[2] Working principles

The network consists of collection nodes which are interconnected each other in the distributed manner that helps to obtain the output from the given inputs. The network works according to the concept of the brain functions and activities which is done by using three different layers such as input, hidden and output layer. The input layer obtains input from the previous feature extraction step, which is passed to the next hidden layer via the connected links

In addition to this network consists of collection of weights and bias value that helps to calculate the output value with effective manner. In hidden layer, the received inputs are process and fed into the output layer in which the output is calculated as,

$$Net\ output = \sum_{i=1}^{N} x_i * w_i + b \ldots$$

At the time of output estimation process, the network trains the features using the training

algorithm in this work, the Levenberg-Marquardt learning algorithm has been utilized for updating the weights and bias value which is done the equation

$$X_{k+1} = X_k - [J^T J + \mu I]^{-1} J^T$$

This training process produces the related output for all the features present in the neural networks. In the testing phase, the query template feature is compared to the output of the neural network, when it replies 0 the template is normal else it has been considered as the skin cancer related features. According to the concept of the traditional Artificial Neural Network working process in this work, Single Layer Artificial Neural Network and Multi-Layer Neural Network has been used for making the effective skin cancer classification process.

[3] Delta Learning Rule

One of the effective functions of the learning rule is minimizing the error rate while examining the extracted features [11]. The delta learning rule that mostly uses the gradient descent learning process which helps to update the weights present in the Single Layer Artificial Neural Networks. Then the delta rule of the neuron weights has been defined as,

$$\Delta w_{ji} = \alpha(t_j - y_j) g'(h_j) x_i \ .$$

According to the above process, the delta learning rule is applied to the network for minimizing the error rate with effective manner. The minimized error rate also improves the recognition rate while analyzing the extracted features. In our research work, Delta learningrule has used inprocess of classification.

[4] Linear ANN

The modelling of the proposed PHC is elucidated in this section. The extracted feature set is provided as an input to the proposed 70 hybrid classifier for performing the recognition of the spliced. The three main classification modules of the modelled classifier are the ANN classifier, DT classifier and the probabilistic model-based classifier. The generated classes from the DT and ANN classifier are utilized by the probabilistic model-based classifier. This hybrid classifier recognizes the optical spliced on the basis of the maximum posterior probability measure representing the spliced image.

The ANN classifier adopted here utilizes the FLM training algorithm [16] developed by the integration of the firefly optimization algorithm with the LM algorithm. The detailed discussion on the series of steps adopted

during the weight update in the FLM based ANFIS. The spliced image's feature vectors [f]=mx F are classified into any one of the 62 classes. Each matrix formatted input feature vector comprises of the vector space values categorized into classes in accordance with the feature space splice distils. The generated classes are mentioned as the mutually exclusive labels. The NN classifier output for the n number of the input image is represented as equation

$$(F \times 1) = C_o; 1 \le o \le 62$$

Here, o is the output class, Output generated by the NN classifier is denoted as Co

The system performs the splice image detection using the fusion of features and applied to the ANN classification purpose. It also represents the individual ANN classification operation on different features, then depending upon the classification accuracy the majority voting operation will be performed and maximum accuracy features with results output as high accuracy spliced image.

IV. PROPOSED SYSTEM

To detect the slicing region in digital image we have to perform edge detection, error analysis, deep learning mechanism [20] to achieve the goal. In our research for the edge detection, we develop Sobel operator, to make the edge detection operation as powerful here we designed gaussian low pass filter for error analysis. Subsequently we will perform the

deep learning algorithm as GARIC (Generalized Approximate Reasoning based Intelligence Control) with regression rules for feature extraction, feature matching and post processing, at the result the detection rate is obtained in figure below.

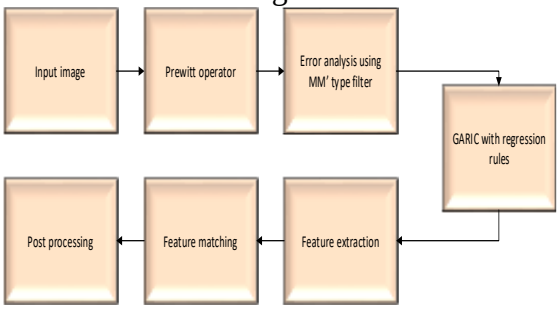

Figure 3. Proposed methodology

The key contribution of our proposed research is summarized below,

- Initially train the input image
- Do the error analysis and edge detection with the use of MM[1] type filter and Prewitt operator.
- Design deep learning algorithm, GARIC with regression rules
- Perform feature extraction and feature matching with the help of deep learning algorithm.
- At last, detect the copy move forgery in digital image.

To improve the splicing detection rate and accuracy with state of art techniques, all the local features (color, texture, and shape) are optimized to construct the feature vector due to their richness in the content information. The proposed optimized splicing detection system framework is shown in Figure 3. All the color images including the query image are converted into HSV color space. The Hue and Value components are quantized to appropriate levels to extract the maximum color information from the image. Here, the Hue and Value are quantized to 18/36 and 10/20 levels respectively and corresponding histograms are constructed. The quantization level 18 makes the Hue divided into 20 parts where each bin in the H- histogram represents 200 ranges of colors and quantization level 36 makes Hue divided into 10 parts where each bin in the H-histogram represents 100 ranges of colors. More number of bins in the histogram provides annoying discrimination in between the relative intensity and brightness of pixels. In this thesis maximum number of bins used for H-histogram is 18 and S-histogram is 10

All these histograms are concatenated to construct a feature vector for all databases and query images. Finally, based on the analysis of similarity metric values images are retrieved and indexed.

The proposed method has been taken the HSV color model due its descriptive nature of brightness and intensity of color. The Hue (H) and Saturation (S) components are quantized to appropriate levels i.e., H can be quantized for 18/36 and S can be quantized for 10/20 (as explained in Chapter-3) based on image size in the database. CMS-LBP [11] applied on value space for texture features using LQP structure which is shown in Fig. 5. It has been observed that more quantization levels on H & S components give the greater number of unwanted features. These features create the more distance between adjacent colours. Based on this criterion small size images undergo on 36 & 20 quantization levels The following steps demonstrate the procedure of proposed image retrieval system.

1. All the database images including query image are converted into HSV color space from RGB color space.
2. Based on the size of an image of a particular database appropriate quantization level has been chosen and the histograms are constructed for H & S components individually.
3. Take a 5x5 pattern which is shown in Fig.2, from a value space.
4. Compute local differences for centre pixel.
5. Calculate 16-bit CMS-LBP pattern for a centre pixel which has been taken.
6. Shift the centre pixel and repeat step-4 &5 for all pixels in the image.
7. Construct histogram for all CMS-LBP patterns.
8. In order to build feature vector database, concatenate all histograms (H, S, & V).
9. Apply similarity metric between query and

database images using to retrieves and index the images.

Feature Extraction using HOG

HOG descriptor which employed here for the feature extraction. The two computation units considered here are the cells and blocks. Initially, the input image is divided into small regions known as cells. In every cell, the edge orientations or histogram of gradient directions is estimated for each pixel. After this, the normalization of all the histograms is done for enhancing the accuracy. The evaluation of normalization is done by measuring the intensity of a group of cells termed as blocks. The HOG feature extraction process is depicted in Figure 4.

Initially, the pre-processed image is split into g number of cells. The size of each cell is Y×X ; each cell comprises of X*Y number of pixels. Then, the histogram is computed for each cell. Following this, the cells are grouped for the generation of r number of blocks. Hence, the normalization is done to every image block. In Figure 6, if the size Pre-processed Image Block Partitioning Histogram Gradient Computation Gradient Vote Feature Vector Normalization Block 96 of each cell is 4×4 size, then, the size of the block is represented as 16×16. The HOG feature extraction process is elaborated in the upcoming steps.

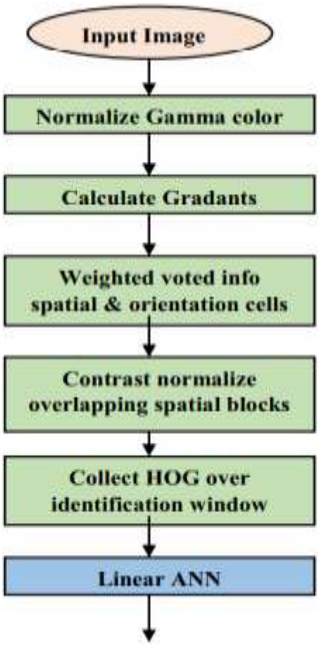

Figure 4: Splicing Image Forgery feature extraction process and object identification procedure

1. Gradient Estimation

The magnitude and orientation of each pixel (x, y) in the cell are estimated. Consider that the pixel is located at the (x, y) coordinate and its luminance value is indicated as l(x, y) . Then, the pixel's horizontal and vertical gradients are expressed as shown in equations.

$$I_x(x,y) = l(x+1,y) - l(x-1,y)$$

$$I_y(x,y) = l(x,y+1) - l(x,y-1)$$

The magnitude m(x, y) developed by Olarik et al. (2015) is expressed as shown in equation

$$m(x,y) = \sqrt{I_x(x,y)^2 + I_y(x,y)^2}$$

Then, the orientation is estimated by using equation,

$$\theta(x,y) = \arctan\frac{I_x(x,y)}{I_y(x,y)}$$

2. Gradient Vote

The gradient vote of an orientation histogram is validated regarding the gradient element centered within the cell. After this, the 97 determined orientation is spitted into a number of bins. The equations formulated for

Industrial Engineering Journal
ISSN: 0970-2555
Volume : 52, Issue 2, No. 1, February : 2023

incrementing the two bins a–1 and a are expressed in the equations accordingly,

$$v_1 = (1-a)*m(x,y)$$

$$v_2 = a*m(x,y)$$

Here, the pixel weight is denoted as a and the magnitude is indicated as .) , (m x y The pixel weight is estimated using the below equation

$$a = (c+0.5) - \frac{b*\theta(x,y)}{\pi}$$

Here, the number of bins is denoted as b and the bin having the orientation (x, y), θ is denoted as c. Eventually, the normalization of each block is evaluated.

3. Normalization Computation

The normalization of each block consisting of number of histogram cells is estimated. The normalization expression for each block is shown in below equation

$$n_u^c = \frac{n_u}{\sqrt{\|n\|_2^2 + \sigma^2}}$$

Here, the combined histogram cell's block vector is indicated as u n and the constant, whose limit varies from one to b×g, is denoted as u and the small constant for restricting the infinite constraint is notified as σ. Hence, the feature vector F is created by gathering the HOG descriptor feature from all the image blocks.

V.SIMULATION RESULTS

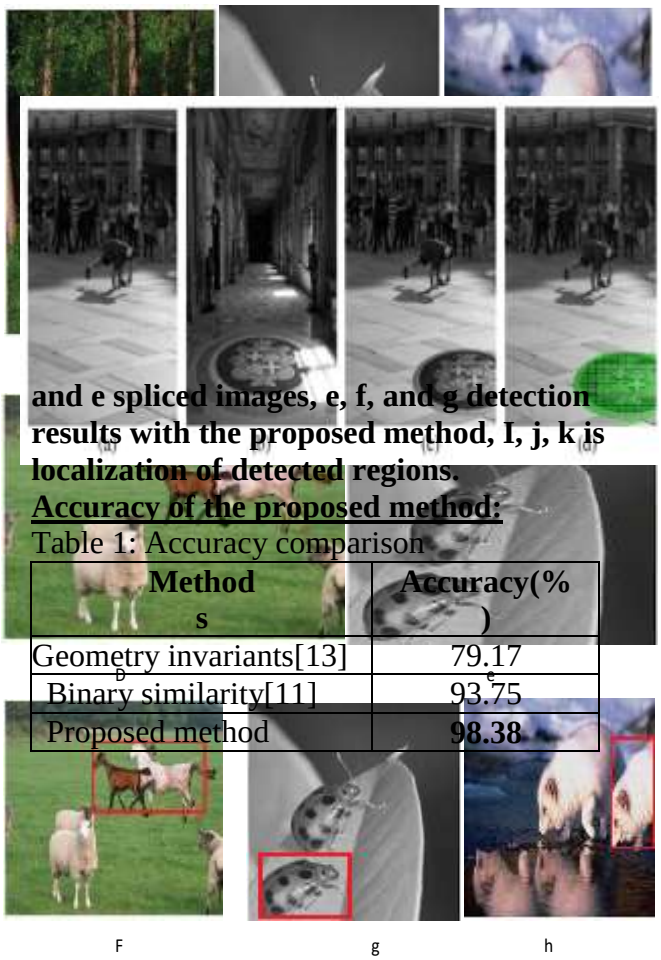

and e spliced images, e, f, and g detection results with the proposed method, I, j, k is localization of detected regions.

Accuracy of the proposed method:

Table 1: Accuracy comparison

Methods	Accuracy(%)
Geometry invariants[13]	79.17
Binary similarity[11]	93.75
Proposed method	**98.38**

I.

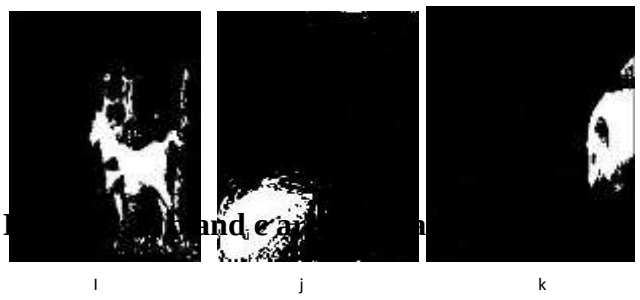

Figure 6: a and b are original images c spliced image and d detection of spliced region.

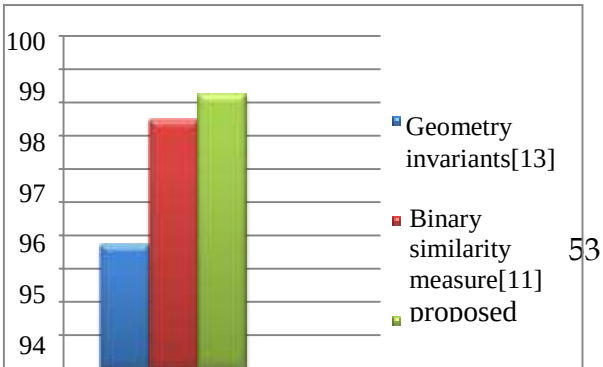

Figure 7: Graphical representation of Accuracy.

VI.CONCLUSION

Digital image splicing detection is a process of detecting, storing, analysing and presenting evidence from the source. Spliced images will lead series of threats in image security as well as destroy someone's reputation in the society. Hence, development of an automatic splicing detection model becomes important to effectively analyse the trustworthiness of an image. Intrusive and non-intrusive are the two techniques used to authenticate image content. Developing an automatic non-intrusive splicing detection [19] algorithm to ensure reliability of an image is most prominent research area in image processing. Image splicing detection has higher influence in different domains such as forensic investigation, law enforcement, insurance claim processing, scientific journals and wherever images are used as evidence.

In this research work importance of digital image splicing detection and its implementation issues have been discussed. Experimental analysis on various splicing detection methods are carried out and optimized nonintrusive image splicing detection model has been developed by using an efficient block and key point descriptors. Images are processed in spatial and frequency domains. Processing images in spatial domain incurred more computation and makes the image processing task a complex one. Hence, a new block-based copy-move splicing detection approach has been developed by using

This method has lower computational complexity and high accuracy rate over the existing methods but not suitable for spatial feature-based analysis.

An efficient splicing detection algorithm has been developed based on ANN to discover simple and multiple spliced regions even after some geometric and image distortions. Results show that this method performs better than existing SIFT and SURF methods. Selection of optimum features from the extracted features is another significant phase in any splicing detection approach. An efficient method has been developed GARIC features to classify the spliced image from the original image through ANN classifier. Empirical outcome demonstrate that this method performs well than existing methods by means of accuracy, specificity and sensitivity.

VII. REFERENCES

[1] H. Farid, "A Survey of Image Forgery Detection", Signal Processing Magazine, vol. 26(2), pp: 16–25, 2009.

[2] Gajanan K Birajdar, Vijay H Mankar, "Digital image forgery detection using passive techniques: A survey", Digital Investigation, Vol.10 (1), pp: 226–245, Elsevier, 2013.

[3] Luo Weiqi, Qu Zhenhua, Pan Feng, Huang Jiwu, "A survey of passive technology for digital image forensics", Frontiers of Computer science, Vol.2 (1), pp: 1−11, 2007.

[4] Tanzeela Qazi, Khizar Hayat, Samee U Khan, Sajjad A Madani, Imran A Khan, Joanna Kołodziej, Hongxiang Li, Weiyao Lin, Kin Choong Yow, Cheng-Zhong Xu, "Survey on blind image forgery detection", IET Image Processing, Vol.7(7), pp:1–11, 2013.

[5] V. Thirunavukkarsu, J. Satheesh Kumar, "Analysis of digital image forgery detection techniques", International Conference on Convergence Technology, Vol.4 (1), pp: 1000–1002, 2014.

[6] V. Thirunavukkarsu, J. Satheesh Kumar, "Analysis of various noise models and filtering techniques used for image restoration", IJRCSIT, Vol.3 (1), pp: 4–9, 2014.

[7] C. Rey, J.L. Dugelay, "A survey of watermarking algorithms for image authentication", EURASIP Journal on applied Signal Processing, Vol.2 (6), pp: 613–621, 2002.

[8] Pointcheval, J.Stern, "Security arguments for digital signatures", Journal cryptography, Vol.13 (3), pp: 361-396, 2000. [9] Thirunavukkarasu, J.Satheesh Kumar, "Intrusive and Non-Intrusive Techniques for Detecting Fake Images", IJBI, Vol.3 (1), pp: 374 – 379, 2014.

[10] Ng, Chang, S.F.Lin, C. Y.Sun, "Passive-blind

a

image forensics", Multimedia Security Technologies for Digital Rights, Vol.15(1), pp:383-412, 2006.
[11] Bayram S, Avcibas I, Sankur B, Memon N, "Image manipulation detection with binary similarity measures", In IEEE Signal Processing Conference, pp:1-4, 2005.
[12] Thirunavukkarasu V, Satheesh Kumar J, "Evolution of blind methods for image splicing detection-A review", International Journal of Applied Engineering Research, Vol.9 (21), pp: 5069–76, 2014.
[13] Yu-feng Hsu, Shih-fu Chang, "Detecting Image Splicing using Geometry Invariants and Camera Characteristics Consistency", ICME, pp: 549-552, 2012.
[14] Lin, Zhouchen, "Detecting doctored images using camera response normality and consistency", Computer Vision and Pattern Recognition, Vol. 1(1), pp: 1087-1092, 2005.
[15] Hsu, Yu-Feng, Shih-Fu Chang, "Image splicing detection using camera response function consistency and automatic segmentation", 2007 IEEE International Conference on Multimedia and Expo, 2007.
[16] Yu-Feng Hsu, Shih-Fu Chang, "Camera Response Functions for Image Forensics: An Automatic Algorithm for Splicing Detection", IEEE Transactions on Information Forensics and Security, Vol. 5(4), pp: 816-825, 2010.
[17] Johnson M, Farid H, "Exposing digital forgeries through chromatic aberration", In: Proc.ACM Multimedia and security workshop, 2006.
[18] IdoYerushalmy, Hagit Hel-Or, "Digital Image Forgery Detection Based on Lens and Sensor Aberration", International journal of computer vision, Vol.9(2), pp:71–91, Springer, 2011.
[19] Ahmet Emir Dirik, Nasir Memon, "Image Splicing Detection Based on Demosicing Artifacts", IEEE Transaction on Signal processing, Vol.1(1), pp: 1497-1500, 2009.
[20] Choi, Chang Hee, HaeYeoun Lee, Heung Kyu Lee, "Estimation of color modification in digital images by CFA pattern change", Forensic science international, Vol. 226(1), pp: 94-105, 2013. Please purchase PDF Split-Mer
[21] Lu Li, JianruXue, Xiaofeng Wang, Lihua Tian, "A robust approach to detect digital forgeries by exploring correlation patterns", Pattern Analysis and Applications, Vol.18(2), pp:351–365, Springer, 2013.
[22] R. Gonzalez and R. Woods, 2002 "Digital Image Processing" 3rd Edn., Prentice Hall Publication, ISBN:9788120336407
[23] M.R.Banham, A.K.Katsaggelos, "Digital image restoration", IEEE Signal Processing Magazine, vol. 14, pp: 24-41, 1997.
[24] Jain, Anil K, "Fundamentals of digital image processing", Prentice-Hall, 1989.
[25] C.L.Chan, A.K.Katsaggelos, A.V. Sahakian, "Image sequence filtering in Quantumlimited noise with applications to low-dose fluoroscopy", IEEE Transaction on Medical Imaging, Vol. 12, pp. 610-621, 1993.